Supercurrent Spectroscopy of Andreev States

L Bretheau, C Ö Girit, C Urbina, D Esteve, H Pothier

Supercurrent Spectroscopy of Andreev States

L. Bretheau*, Ç. Ö. Girit*, C. Urbina, D. Esteve and H. Pothier[a]

*Quantronics Group, Service de Physique de l'État Condensé (CNRS,
URA 2464), IRAMIS, CEA-Saclay, 91191 Gif-sur-Yvette, France*

(Dated: January 7, 2014)

We measure the excitation spectrum of a superconducting atomic contact. In addition to the usual continuum above the superconducting gap, the single particle excitation spectrum contains discrete, spin-degenerate Andreev levels inside the gap. Quasiparticle excitations are induced by a broadband on-chip microwave source and detected by measuring changes in the supercurrent flowing through the atomic contact. Since microwave photons excite quasiparticles in pairs, two types of transitions are observed: Andreev transitions, which consists of putting two quasiparticles in an Andreev level, and transitions to odd states with a single quasiparticle in an Andreev level and the other one in the continuum. In contrast to absorption spectroscopy, supercurrent spectroscopy allows detection of long-lived odd states.

I. INTRODUCTION

The Josephson supercurrent between two superconductors [1] exists in all types of weak links, including tunnel junctions, constrictions, molecules, and normal metals. Weak links differ one from another by their quasiparticle excitation spectrum, which is determined by the length of the weak link and the transmission probabilities τ_i for electrons through each conduction channel i. In tunnel junctions, $\tau_i \ll 1$, and all excitations conserving electron parity require energies at least equal to 2Δ, where Δ is the superconducting gap energy. With energy 2Δ, a pair can be broken and two quasiparticles created at the gap energy Δ. This is the same situation as in a bulk superconductor. In contrast, the excitation spectrum of weak links that have well transmitted channels, such as superconducting constrictions, contains sub-gap spin-degenerate Andreev levels (Andreev doublets) (see Fig. 1a). The energy of the Andreev level associated with one channel with transmission τ in a short weak link is $E_A = \Delta\sqrt{1 - \tau \sin^2\left(\delta/2\right)}$ [2, 3], with δ the superconducting phase difference across the weak link. The lowest energy excitation that conserves electron parity, the "Andreev transition", has an energy $2E_A$: it consists in the creation of two quasiparticles in the Andreev level (red double arrow in Fig. 1a), which can be thought of as the excitation of a pair localized at the weak link [4, 5]. We recently reported microwave spectroscopy of this Andreev transition in superconducting atomic contacts [4]. There is a second type of excitation, with energy at least $E_A + \Delta$, in which a localized Andreev pair is broken into one quasiparticle in the Andreev level and one in the continuum (green arrows in Fig. 1a). This process was addressed theoretically in recent works [6–8], but has never been observed experimentally. Here, we describe how "su-

---

[a]Corresponding author : hugues.pothier@cea.fr; *L. Bretheau and Ç. Ö. Girit contributed equally to this work.
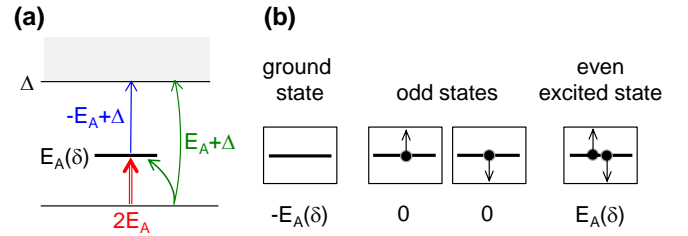
Figure 1: **(a)** The single particle excitation spectrum for each channel of a weak link consists of a doubly-degenerate Andreev level at energy $E_A\left(\delta\right)$, and a continuum of states at energies larger than the superconducting gap Δ. Arrows indicate transitions that can be induced by microwaves. The four possible occupations of the Andreev level are shown in **(b)**: they correspond to the ground state, the two odd states, and the excited pair state, with energies $-E_A$, 0 and E_A.

percurrent spectroscopy" reveals all possible transitions involving Andreev states (Fig. 1). This method is based on measuring the supercurrent through a weak link and detecting changes induced by microwave excitation [9].

The supercurrent in a weak link results from the phase-dependence of its energy, which depends on the occupation of the Andreev levels. In the case of a single channel (see Fig. 1b), the ground state, with energy $-E_A$, carries a supercurrent $-I_A = -\varphi_0^{-1}\left(\partial E_A/\partial\delta\right)$. The energy of an odd state, with a single Andreev excitation, is zero: it carries no supercurrent. The excited pair state with two Andreev excitations has energy $+E_A$, and therefore carries a supercurrent $+I_A$. This difference in the supercurrent associated with 0, 1 or 2 Andreev excitations is the elementary phenomenon to understand microwave- or voltage-induced variations of the supercurrent [10, 11] as well as the current response to an a.c. field [12] in diffusive superconductor–normal-metal–superconductor junctions [13]. Measurements of the phase dependence of the supercurrent through atomic contacts with a few conduction channels revealed the spontaneous excitation to odd states and allowed characterization of their dynam-

ics [14]. We use here the dependence of the supercurrent on the occupation of the Andreev doublet to reveal the complete excitation spectrum of an elementary, generic weak link: an atomic contact.

II. EXPERIMENTAL SETUP

The experimental setup is shown schematically in Fig. 2a. An atomic contact is obtained by breaking in a controlled manner a suspended constriction in an Al film ($\Delta = 180\,\mu\text{eV}$) [5, 15]. It is placed in parallel with a tunnel Josephson junction having a much larger critical current $I_0 \simeq 1.06\,\mu\text{A} \gtrsim 20\,|I_A|$, hence forming an asymmetric SQUID. The number of conduction channels in the atomic contact and their transmission probabilities are determined from a fit of the current-voltage characteristic of the SQUID [16]. The magnetic flux ϕ through the SQUID loop fixes the phase difference at the atomic contact to $\delta = \varphi + \gamma$, with $\varphi = 2\pi\phi/\phi_0$ the reduced flux, $\phi_0 = h/2e$ the flux quantum, and γ the phase across the SQUID junction. The SQUID is asymmetric enough so that $\gamma \simeq \arcsin(I_b/I_0)$ is determined only by the bias current I_b. The SQUID is capacitively coupled on-chip to a small Josephson junction (critical current $48\,\text{nA}$), called the "emitter". Figure 2b shows a micrograph of the SQUID and the emitter. The emitter is biased at a voltage V_J and due to the a.c. Josephson effect acts as a broadband microwave source at frequency $\nu_J = 2eV_J/h$. When $h\nu_J$ matches a transition energy in the atomic contact, a photon can be absorbed, and the occupation of Andreev states is modified. In "absorption spectroscopy" experiments performed on the same device [4], energy dissipated during excitation of an Andreev transition in the superconducting atomic contact was detected by measuring the d.c. current through the emitter. Here instead, the corresponding change in the supercurrent $I_{AC}(\delta)$ of the atomic contact is accessed by measuring the critical current of the SQUID: to a good approximation, the critical current of such an asymmetric SQUID is the sum of the critical current I_0 of the SQUID Josephson junction and of $I_{AC}(\delta)$.

In practice, due to thermal fluctuations, the SQUID switches to a finite voltage state at a current inferior to the critical current. The current $I_{AC}(\delta)$ is therefore inferred from the switching probability $P_{sw}(I_b)$ when a bias current pulse of height I_b and duration $t_p = 1\,\mu\text{s}$ is applied (Fig. 2c) [17]. The probability $P_{sw}(I_b)$ increases smoothly from 0 to 1 around the switching current, which is I_{sw}^0 for the junction alone and $\sim I_{sw}^0 + I_{AC}(\delta)$ for the atomic SQUID [16], i.e. $I_{sw}^0 - I_A$ in the ground state, $I_{sw}^0 + I_A$ in the excited state and I_{sw}^0 in the odd states (Fig. 2d&e). The principle of our experiment is to measure changes of P_{sw} induced by the microwave excitation.

The switching probability is calculated from the response to a train of 10^4 pulses. For each value of the flux ϕ, the height of the measurement pulse is set to I_{sw} such that $P_{sw} = 0.5$ in the absence of microwaves, i.e.

at $V_J = 0$. Assuming that the atomic contact is then in its ground state, $I_{sw} = I_{sw}^0 - I_A(\delta)$ (Fig. 2d&e). Then P_{sw} is recorded as a function of the microwave excitation frequency set by V_J. This procedure is repeated for all values of ϕ, and one obtains a map of P_{sw} as a function of φ and V_J : the "switching spectrum". Such a spectrum is shown in Fig. 3a for a contact with two channels of significant transmissions: $\tau_1 = 0.985$, $\tau_2 = 0.37$. Most of the features of the rich spectrum, which has numerous phase- and energy-dependent lines and plateaus, are explained below and in the Supplemental Material [18].

III. INTERPRETATION OF THE SPECTRUM

We first discuss general aspects of the spectrum which are unrelated to Andreev physics. The white band slightly above $2eV_J \simeq 0.5\Delta$ with no data corresponds to voltages that cannot be accessed due to an instability in the I-V of the emitter when the Josephson frequency matches the plasma frequency ν_p of the SQUID [4]. When $2eV_J > h\nu_p$, the background of the image is light blue, corresponding to an overall increase of the switching probability to $P_{sw} \simeq 0.55$ interpreted as an increased noise temperature when the emitter is biased. When $2eV_J < h\nu_p$, the overall increase in P_{sw} is even stronger ($P_{sw} \simeq 0.6 - 0.8$), with broad, phase-independent stripes in the spectrum, corresponding to a $10 - 20$ mK increase in the effective temperature, an effect attributed to resonant activation during the measurement pulse [9, 19].

A. Identification of the transition lines

Relevant to the physics of Andreev levels are changes in P_{sw} that depend on the phase across the atomic contact. They are better seen in Fig. 3b, where the slow components of $P_{sw}(V_J)$ in Fig. 3a have been filtered out to obtain δP_{sw} (the signal was first smoothed on 0.17Δ-intervals; the result was then subtracted from the original spectrum). Three types of transitions are resolved, corresponding to the arrows in Fig. 1a: the Andreev transition, i.e. the excitation of the Andreev pair (red arrow); the transition to an odd state with a single quasiparticle in the Andreev doublet, the second one being excited to the continuum (green arrows); the excitation of a quasiparticle from the Andreev level to the continuum (blue arrow).

Andreev transitions at $2eV_J = 2E_A$ (red arrow in Fig. 1a) are seen as sharp V-shaped lines centered at $\varphi = \pi$, with minima at $2E_{A1}(\pi) \simeq 0.25\Delta$ for the channel with transmission $\tau_1 = 0.985$ and $2E_{A2}(\pi) \simeq 1.6\Delta$ for the channel with transmission $\tau_1 = 0.37$ (red lines in Fig. 3c). The variations across the spectra of the intensity of the lines are discussed in the Supplemental Material [18].
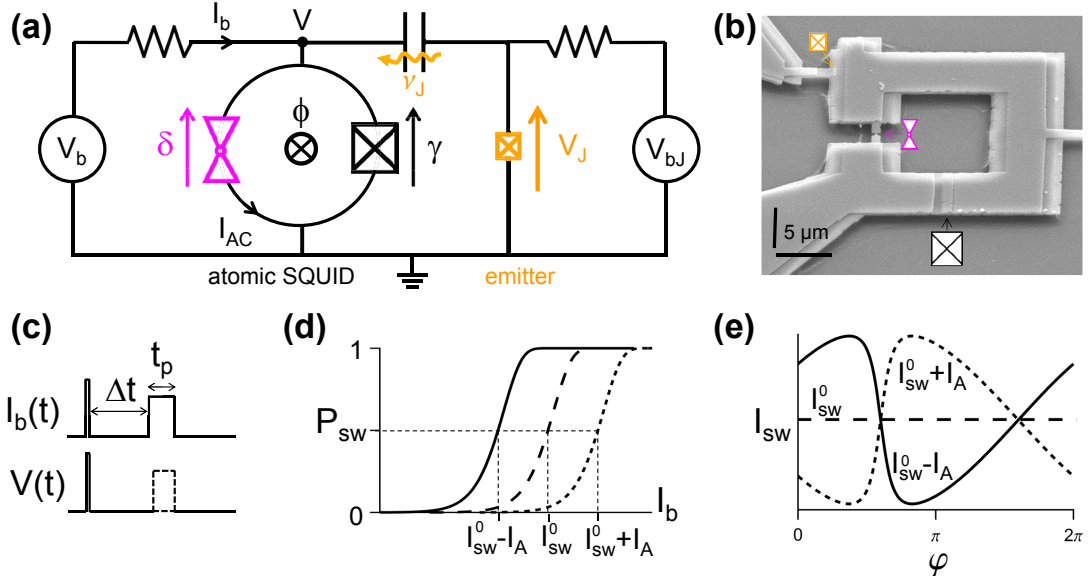
Figure 2: **(a)** Simplified schematic of the experimental setup. An asymmetric SQUID is formed by an atomic contact (magenta triangles) and an ancillary Josephson junction (critical current $I_0 \simeq 1.06\,\mu\text{A}$, 20 times larger than the typical critical current of a one-atom aluminum contact). In the absence of SQUID bias current ($I_b = 0$), magnetic flux ϕ threading the loop imposes a phase $\delta \simeq \varphi \equiv 2\pi\phi/\phi_0$ across the contact and determines its excitation spectrum and the loop current I_{AC}. It is coupled through a capacitor to a voltage-biased Josephson junction (yellow checked box, critical current $48\,\text{nA}$) used as an emitter: when biased at voltage V_J, it produces an a.c. current at Josephson frequency $\nu_J = 2eV_J/h$. **(b)** Micrograph of the sample, seen under an angle (scale bars indicate $5\,\mu\text{m}$ in two directions). **(c)** The SQUID switching current is measured by applying sequences of current (I_b) pulses of duration t_p. A time Δt before each measurement pulse, any memory of the response to the previous pulse is erased by a strong current pulse ("prepulse") that forces the SQUID to switch [14]. Switching events are detected by the appearance of a voltage V across the SQUID. **(d)** Sketch of the switching probability P_{sw} of the atomic SQUID as a function of the bias current I_b, for the atomic contact in its ground state (solid line), in an odd state (dashed line) and in the excited pair state (short-dashed line). For this figure, we assumed a single channel and $I_A > 0$. The switching current of the SQUID Josephson junction in the absence of an atomic contact is I_{sw}^0. **(e)** Sketch of the switching current of the SQUID as a function of the phase φ in the ground, odd or excited even states.

There are in addition two strong lines parallel to $E_{A1}(\delta)$ and two faint lines parallel to $E_{A2}(\delta)$ in the spectrum (magenta lines in Fig. 3c). They correspond to exciting Andreev transitions with the second harmonic of the Josephson frequency. We do not understand however why the lines are shifted up or down with respect to the expected position $2eV_J = E_{Ai}$ by a few µV.

Transitions from the ground state to an odd state with one quasiparticle in the Andreev doublet (energy E_A), and another one at energy larger than Δ in the continuum (green arrows in Fig. 1a and green lines in Fig. 3c) are best seen in the first channel as a reduced P_{sw} (white in Fig. 3a) in a region defined by $2eV_J > E_{A1} + \Delta$. The corresponding threshold for the second channel is also seen at $2eV_J = E_{A2} + \Delta$.

There is a faint transition at $2eV_J = -E_{A1} + \Delta$ (blue line in Fig. 3c). It corresponds to exciting a quasiparticle from the Andreev doublet of the first channel to the continuum (blue arrow in Fig. 1a). The detection of this odd-even transition is explained if one assumes a finite probability that the doublet is occupied in the absence of excitation (as already found in former experiments [14]).

Blurred replica of the transition lines are visible shifted leftwards by $\sim 0.4\pi$. They correspond to transitions induced not before, but during the measurement pulse, as the microwave produced by the emitter is applied continuously. During the pulse, a finite current flows through the SQUID junction and the phase across the contact is no more $\delta = \varphi$, but $\delta = \varphi + \gamma_{\text{sw}}$ with $\gamma_{\text{sw}} \simeq \arcsin\left(I_{\text{sw}}^0/I_0\right) \sim 0.4\pi$. The replica of the odd-even transition discussed in the previous paragraph is responsible for the sharp disappearance of the Andreev transition line at $\varphi \gtrsim 1.04\pi$, as discussed in the SM [18].

B. Sign of changes in P_{sw}

In most of the spectrum ($0.6\pi < \varphi \lesssim 1.5\pi$) the Andreev transitions and the transitions to odd states manifest themselves by a decrease of the switching probability P_{sw} (white on blue background in Fig. 3a, black on grey background in Fig. 3b). In contrast, the faint odd-even transition gives an increased P_{sw}. At $\varphi \sim 0.6\pi$, all transitions disappear, and reappear at $\varphi < 0.6\pi$ with opposite sign of the change in P_{sw} (this effect is particularly visible on the line at $2eV_J = 2E_{A2}$ and on its replica).
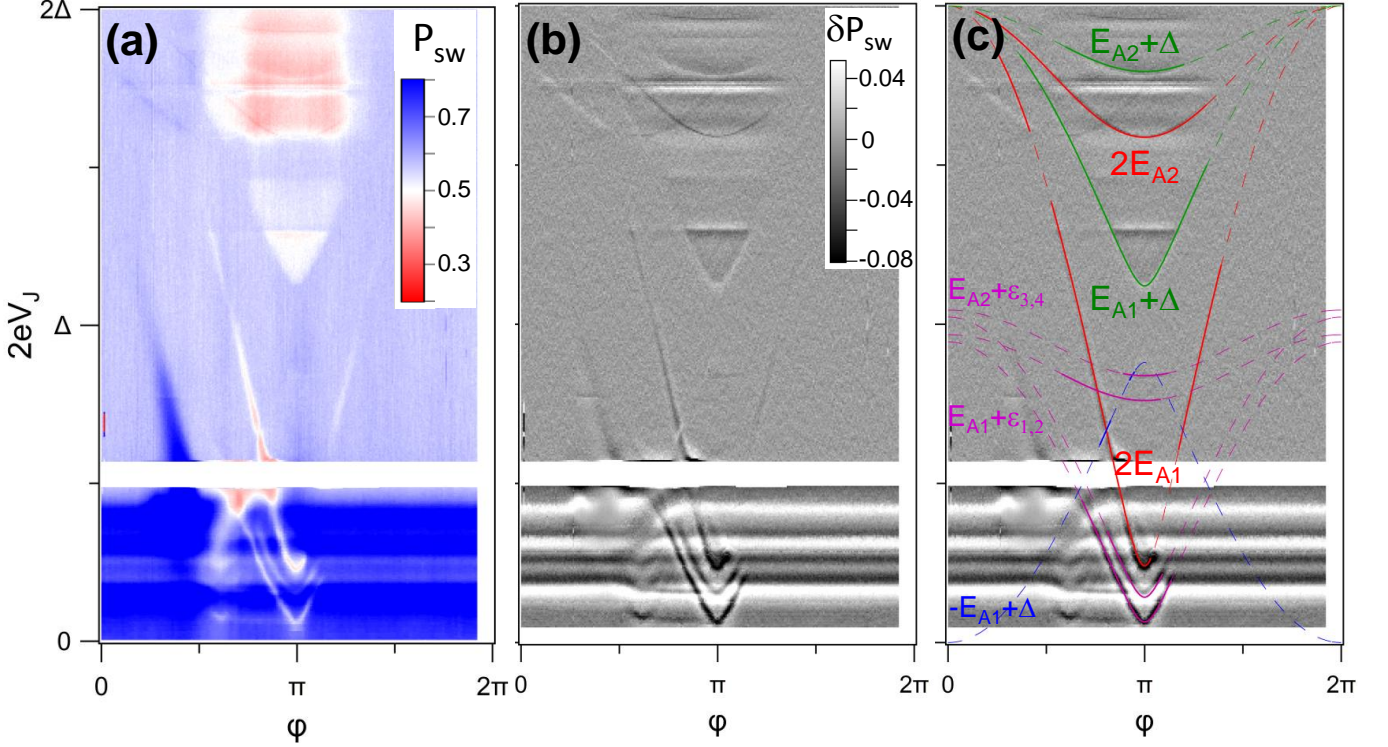
Figure 3: **(a)** Switching spectrum $P_{sw}(\varphi, 2eV_J)$ measured on an atomic contact with two channels of transmissions 0.985 and 0.37. **(b)** Filtered spectrum $\delta P_{sw}(\varphi, 2eV_J)$ (see text) highlights rapid variations of the switching probability with energy. **(c)** Same as (b), with transitions underlined. Dashed lines correspond to the predicted positions of transitions, and solid lines underline where they are actually visible in the data. Colors correspond to those of arrows in Fig. 1a. In red, Andreev transitions at $2eV_J = 2E_{A1,2}$. Green lines: threshold $2eV_J = E_{A1,2} + \Delta$ for transitions odd states with one quasiparticle in an Andreev level, another one in the continuum. Blue line: threshold $2eV_J = -E_{A1} + \Delta$ for transitions from odd states to even states by transferring a quasiparticle from the Andreev level into the continuum. Magenta lines: Andreev transitions induced by the second harmonic of the excitation when $2eV_J = E_{A1,2}$, shifted by energies $\varepsilon_{1-4} = -5, 2, -3, 4\,\mu eV$ (from bottom to top).

The explanation is found in Fig. 2d&e: starting from the ground state (solid lines), all transitions lead to a decrease of P_{sw} in the regions where $I_A(\delta) > 0$. Since $\delta = \varphi + \gamma_{sw}$ during the measurement pulse, $I_A(\delta) > 0$ when $0.6\pi < \varphi < 1.6\pi$.

The odd-even transition (blue line) is seen because of a finite probability to find initially the Andreev level in an odd state. Then the initial pulse height, set such that $P_{sw} = 0.5$ when $V_J = 0$, corresponds to a current between $I_{sw}^0 - I_A$ and I_{sw}^0, and transitions to the ground state cause an increase in P_{sw}.

C. Dynamics of the Andreev levels occupation during spectroscopy

We now analyze more in depth the amplitude of changes in P_{sw} and the nature of the states that are detected in the experiment. When exciting Andreev transitions, one expects that $I_{AC}(\delta)$ changes by $2I_A$, because the supercurrent carried by a channel of transmission τ changes from $-I_A$ to $+I_A$. This turns out not to be the case: setting φ and V_J on the Andreev transition line

$2eV_J = 2E_{A1}$, the curve $P_{sw}(I_b)$ does not show the step corresponding to the excited state (see Fig. 4). An explanation is sketched in Fig. 5: when the Andreev pair is excited, it often decays to its ground state; cycles of excitation/relaxation give rise to a d.c. current through the emitter [4]. But it can also decay to an odd state ("quasiparticle poisoning"), which is long-lived [14]. Just before the measurement pulse, the probability to be in an odd state can therefore be large. When the current increases through the SQUID, the phase across the contact changes by up to γ_{sw}, the Andreev energy changes from $E_A(\varphi)$ to $E_A(\varphi + \gamma_{sw})$ and the excitation is no longer resonant with the Andreev transition. The population of the excited state then decays at a rate Γ_r. If $\Gamma_r > t_r^{-1}$ ($\Gamma_r > 10\,\text{MHz}$) with $t_r \simeq 0.1\,\mu s$ the rise-time of the measurement pulse, it relaxes before the pulse has fully developed and no change is detected in P_{sw} [20]. In contrast, the odd state is observed because its decay rate is in general much smaller [14, 21]. Hence, quasiparticle poisoning acts as a "sample and hold" mechanism for detecting Andreev transitions. Note that transitions at energies greater than $E_{Ai} + \Delta$ (green in Fig. 1a and 3c) leave the Andreev doublet directly in an odd state, and
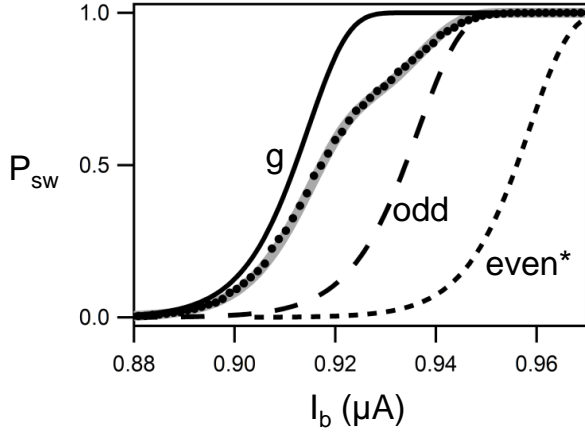
Figure 4: Dots: Switching probability $P_{\rm sw}\left(I_b\right)$ measured near the minimum of the Andreev transition line at $2E_{A1}$ ($2eV_J = 0.24\Delta$, $\varphi = 1.02\pi$). Solid line: calculated $P_{\rm sw}\left(I_b\right)$ with the two channels in the ground state (corresponding to a total current in the SQUID junction $I_b - I_{A1} - I_{A2}$). Dashed line: calculated $P_{\rm sw}\left(I_b\right)$ with the first channel in an odd state (corresponding to a total current in the SQUID junction $I_b - I_{A2}$). Grey curve: fit of the data with sum of the two previous curves with weights 0.63 and 0.37. Short-dashed line: calculated $P_{\rm sw}\left(I_b\right)$ with the first channel in the even excited state (corresponding to a total current in the SQUID junction $I_b + I_{A1} - I_{A2}$). A finite probability to find the channel in the even excited state would have resulted in a contribution of the short-dashed line to the data.

Figure 5: Dynamics of Andreev level occupation in presence of a resonant excitation at frequency $2E_A$. Andreev excitation are induced from the ground state (bottom) to the excited even state (even*, top). When followed by a direct relaxation, the process can immediately repeat itself, and give rise to a d.c. current through the emitter junction, which is the signal used for absorption spectroscopy [4]. Alternatively, one quasiparticle in the Andreev level can recombine with a quasiparticle in the continuum, and lead to an odd state (poisoning). Such states are long-lived, allowing the detection of the preceeding Andreev transition by supercurrent spectroscopy. Odd states relax to the ground state (unpoisoning) by a similar recombination process [22].

their observation does not require quasiparticle poisoning.

For phases such that $\Delta - E_{A1}\left(\varphi + \gamma_{\rm sw}\right) < 2E_{A1}\left(\varphi\right)$, a new process comes into play: unpoisoning by the microwaves during the measurement pulse. Because the Andreev energy approaches Δ due to the phase shift $\gamma_{\rm sw}$, photons at energy $2E_{A1}\left(\varphi\right)$ can excite a quasiparticle from the Andreev level to the continuum during the measurement pulse. This process empties the Andreev level from an odd state and leads to the abrupt disappearance of the Andreev transition line at $\varphi \gtrsim 1.04\pi$ (see Fig. 8 in SM [18]).

When the Andreev doublet is in an odd configuration, energy absorption at $2E_A$ is hindered, and the d.c. current through the emitter associated to the absorption by the Andreev transition is suppressed. This was probed in time-resolved measurements of the emitter current. Quasiparticle poisoning and unpoisoning are then observed in real time as a telegraphic noise in the current, with timescales in the tens of ms (see Fig. 10 in SM [18]).
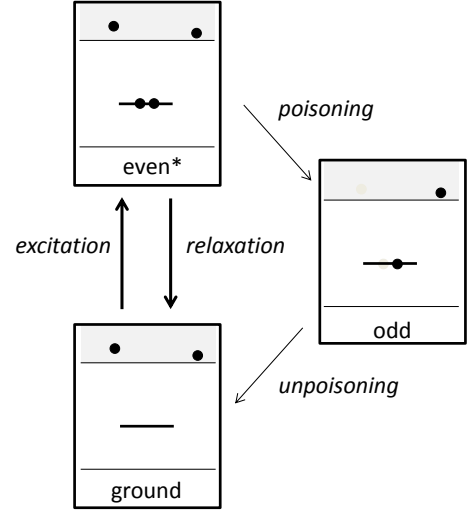
IV. COMPARISON OF ABSORPTION SPECTROSCOPY AND SUPERCURRENT SPECTROSCOPY

Finally, we compare in Fig. 6 the absorption spectrum [4] and the switching spectrum measured on the same atomic contact. The spectra are different because absorption spectroscopy detects excitation/relaxation cycles that repeat themselves rapidly enough to give a substantial current through the emitter, whereas supercurrent spectroscopy requires long-lived states that do not decay during the measurement pulse rise time. Nevertheless, as explained above, transitions to the short-lived even excited states are also seen in supercurrent spectroscopy thanks to quasiparticle poisoning.

The switching spectrum contains more information, in particular in the upper half of the spectrum. Remarkably, the Andreev transition in the second channel ($2eV_J = 2E_{A2}$) which was barely visible in the absorption spectrum is sharply resolved. The switching spectrum does not include the lines associated with the plasma mode of the SQUID at $2eV_J = h\nu_p$, $2h\nu_p$ and $h\nu_p + 2E_{A1}$ (see Fig. 6c), which are apparent in the absorption spectrum. The reason not to see the two first ones is that the lifetime of the plasma mode, estimated to be in the ns range from the quality factor $Q \simeq 22$ of the corre-
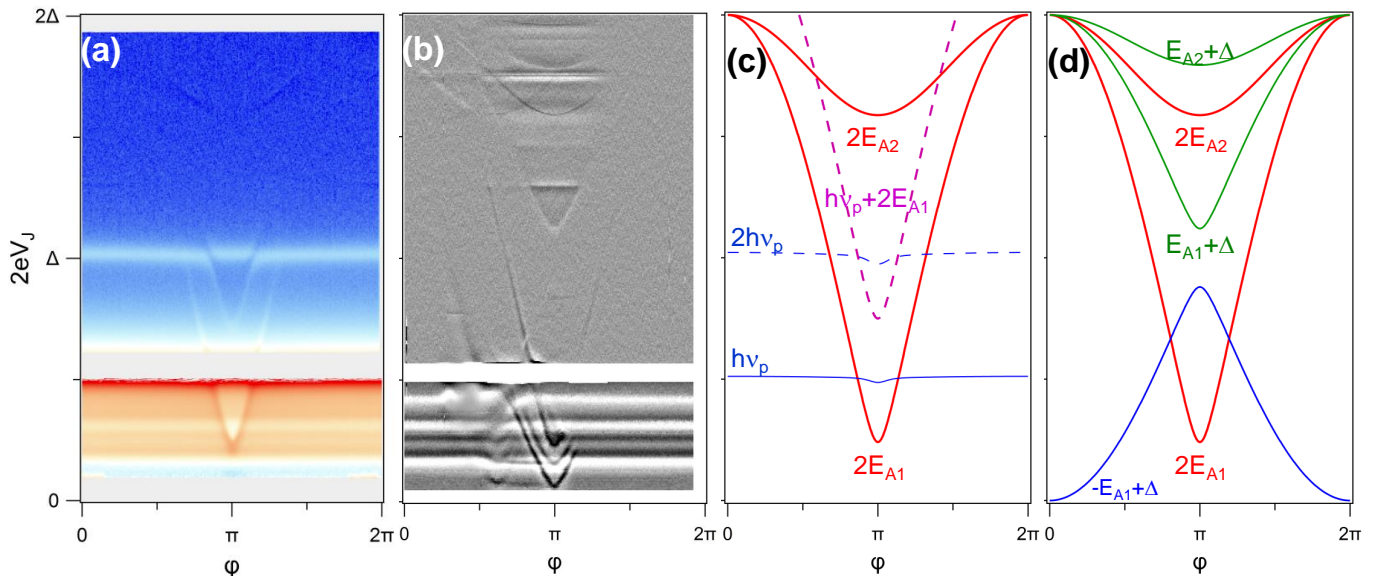
Figure 6: Comparison of the absorption spectrum **(a)** and of the switching spectrum **(b)** taken on the same contact ($\tau_1 = 0.985$, $\tau_2 = 0.37$). **(c)** and **(d)** indicate the main transitions visible in (a) and (b), respectively. Solid red in (c,d): Andreev transitions at $2eV_J = 2E_{A1,2}$. In (c): solid and dashed blue: plasma transition, 1st and 2nd harmonic ($2eV_J = h\nu_p$, $2h\nu_p$); dashed magenta line: simultaneous excitation of Andreev and plasma modes ($2eV_J = 2E_{A1} + h\nu_p$). We also show in (d), with thin green lines, the threshold $2eV_J = E_{A1,2} + \Delta$ for simultaneous excitations of quasiparticles in the Andreev doublet and in the continuum; thin blue line: threshold $2eV_J = -E_{A1} + \Delta$ for transitions from odd states to even states having one quasiparticle in the continuum.

sponding peak in the I-V of the emitter, is much shorter than the rise time t_r of the measurement pulse. However, one would expect to detect the third transition, at $2eV_J = h\nu_p + 2E_{A1}$, which corresponds to a simultaneous excitation of the plasma mode and of the Andreev doublet. We speculate that even if poisoning occurs in the same manner as when $2eV_J = 2E_{A1}$, photons at energy $h\nu_p + 2E_{A1}$ trigger unpoisoning (see SM [18]) and the doublet is found only in its ground state [23].

V.   CONCLUSIONS

The experimental results show that spectroscopy based on the measurement of the Josephson supercurrent allows detecting single quasiparticle excitations in superconducting weak links. The entire excitation spectrum is explained by the presence of Andreev doublets that can be occupied by 0, 1 or 2 quasiparticles. Andreev transitions are detected when followed by quasiparticle poisoning, which acts as a "sample and hold" mechanism by placing the Andreev doublet in a long-lived odd state. We also demonstrate for the first time the possibility to induce, without injecting any charge [24], transitions from the (even) ground state to an odd state with a single excitation in the Andreev doublet (the second one being in the continuum). This type of transition could be used to prepare spin-qubits based on odd states [25, 26].

We thank Alfredo Levy Yeyati, John Martinis and Eva Dupont-Ferrier for discussions. We gratefully acknowl-

VI.   SUPPLEMENTAL MATERIAL

Current-phase relation

In Figure 7, we show the measured switching current of the atomic SQUID, which reveals the current-phase relation of the atomic contact in its ground state [16].

Visibility of the transition lines

Andreev transitions manifest themselves by a decrease of the SQUID switching probability P_{sw} for $\varphi \gtrsim 0.5\pi$, and by an increase of P_{sw} for $\varphi \lesssim 0.5\pi$. They disappear on the right-hand side of the spectrum, for $\varphi \gtrsim 1.4\pi$. The change in the sign of the effect is related both to the shape of the current-phase relation of the atomic contact [Fig. 7 and Fig. 2(e)], which leads to variations of the
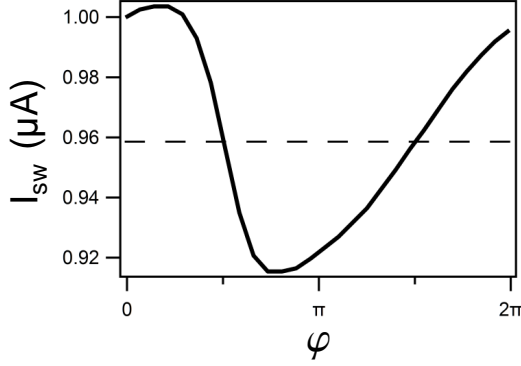
Figure 7: Switching current $I_{\mathrm{sw}} \simeq I_{\mathrm{sw}}^0 + I_{\mathrm{AC}} \left(\varphi + \gamma_{\mathrm{sw}} \right)$ of the SQUID in absence of excitation, defined by $P_{\mathrm{sw}} \left(I_{\mathrm{sw}} \right) = 0.5$ when $V_J = 0$, as a function of reduced flux φ. The horizontal line marks I_{sw}^0.

SQUID switching current around I_{sw}^0, and to the shift of the phase across the atomic contact by

$$\gamma_{\mathrm{sw}} \simeq \arcsin \left(I_b / I_0 \right) \sim 0.4\pi$$

when the current pulse is applied (the equality is exact only in the limit $I_A / I_0 \to 0$). At $\varphi = \pi$, the symmetry point for the system in the absence of current in the SQUID, $I_A = 0$ so that the current through the atomic contact does not depend on the occupation of the ABS. The transition line is nevertheless visible because when the measurement current pulse is applied, the phase δ shifts to $\varphi + \gamma_{\mathrm{sw}} \simeq 1.4\pi$, a phase at which I_A is positive. This is seen in the ground state in Fig. 7, where $I_{\mathrm{sw}} \left(\varphi = \pi \right) - I_{\mathrm{sw}}^0 = -I_A \left(1.4\pi \right) \simeq -0.04 \, \mu\mathrm{A}$. Any transition is therefore expected to increase the switching current, hence decreasing the measured $P_{\mathrm{sw}} \left(I_b \right)$ for fixed measurement pulse height, in agreement with the data. Similarly, transitions induced at $\varphi \sim 0.5\pi$ while $I_b = 0$ are invisible because $\varphi + \gamma_{\mathrm{sw}}$ is close to π during the measurement pulse, and the current through the atomic contact is zero for all configurations, as seen in Fig. 7 where $I_{\mathrm{sw}} \left(\varphi = 0.5\pi \right) \sim I_{\mathrm{sw}}^0$. This explains why the sign of the changes in P_{sw} is that of $I_{\mathrm{sw}} \left(\varphi \right) - I_{\mathrm{sw}}^0$. Finally, the absence of signal for $1.5\pi \lesssim \varphi < 2\pi$ corresponds to the fact that when the measurement pulse is swept up, φ approaches or crosses 2π, so that Andreev levels merge with the continuum where the quasiparticles decay away.

Another remarkable feature of the data is the abrupt disappearance of the $2eV_J = 2E_{A1}$ Andreev transition line when $\varphi \gtrsim 1.04\pi$ (green star in Fig. 8(a)). In this region, microwaves of energy $2eV_J$ can excite quasiparticles from the Andreev doublet to the continuum during the measurement pulse [see Fig. 8(b) and Fig. 8(c)]. Then, the doublet is restored to its ground state and P_{sw} is unaffected. Quantitatively, this requires that the rate W_5 for this process (using the notations of Ref. [8])

is larger than the switching rate of the SQUID when the first channel is in the odd state. To evaluate W_5, two ingredients are needed: the real part of the corresponding admittance $\mathrm{Re} Y_5^{(0)} \left(\omega \right)$ given in Ref. [8] and the amplitude of the phase excitation δ_{ac} due to the emitter. The phase excitation depends on the ratio $x = 2eV_J / h\nu_p(s)$ of the excitation energy and the plasma frequency $\nu_p(s) = \nu_p^0 \left(1 - s^2 \right)^{1/4}$ of the current-biased SQUID ($s = I_{\mathrm{sw}}^0 / I_0 \simeq 0.95$):

$$\delta_{ac} = \left(LI_J^0 / \varphi_0 \right) / \left| 1 - x^2 + jx/Q \right|.$$

Here, $I_J^0 \simeq 48 \, \mathrm{nA}$ is the critical current of the emitter junction, $L \simeq 0.18 \, \mathrm{nH}$ is the parallel combination of the SQUID junction inductance φ_0 / I_0 and of the inductance of the biasing circuit [5] and $Q \approx 22$ is the quality factor of the plasma frequency, evaluated from the line shape of the corresponding peak in the I-V of the emitter junction. At $x = 0$, $\delta_{ac} \simeq 0.03 \, \mathrm{rad}$. Using

$$W_5 = \delta_{ac}^2 \frac{\hbar}{2e^2} \omega \mathrm{Re} Y_5^{(0)} \left(\omega \right)$$

[8], one obtains the unpoisonning probability p_{unpois} of the odd state during the measurement pulse (including the rise time), see Fig. 8(d). This explains why the Andreev lines disappear abruptly when $\varphi \gtrsim 1.04\pi$, corresponding to the threshold for exciting a quasiparticle from the Andreev level to the continuum, and reappears at $\varphi \gtrsim 1.2\pi$ because the rate W_5 diminishes below the MHz range. Note that the same unpoisoning process, which is in principle always possible when $E_A > \Delta/3$ [8], has a negligible probability when $2eV_J = 2E_{A2}$.

Dynamics

The dynamics of the occupation of the Andreev doublet sketched in Fig. 5 was explored for the second channel by varying the delay Δt between prepulse and measurement pulse (Fig. 9). The poisoning rate is too weak to observe transitions to the odd state for short delays ($\Delta t = 1.3 \, \mu\mathrm{s}$) but becomes apparent in a characteristic time of $9 \, \mu\mathrm{s}$.

Absorption spectroscopy measurements on another contact probed the real-time fluctuations between the odd and even occupations of a channel with transmission 0.97 at $\varphi = \pi$. The current-voltage characteristics of the emitter junction shows bistability around $V_J = 32 \, \mu\mathrm{V}$, the voltage corresponding to the Andreev transition at $\varphi = \pi$ (top panel in Fig. 10). The corresponding telegraphic noise on the current (measured with a 5 kHz bandwidth), corresponds to rates of 15 Hz (down rate) and 53 Hz (up rate) (bottom panel of Fig. 10).
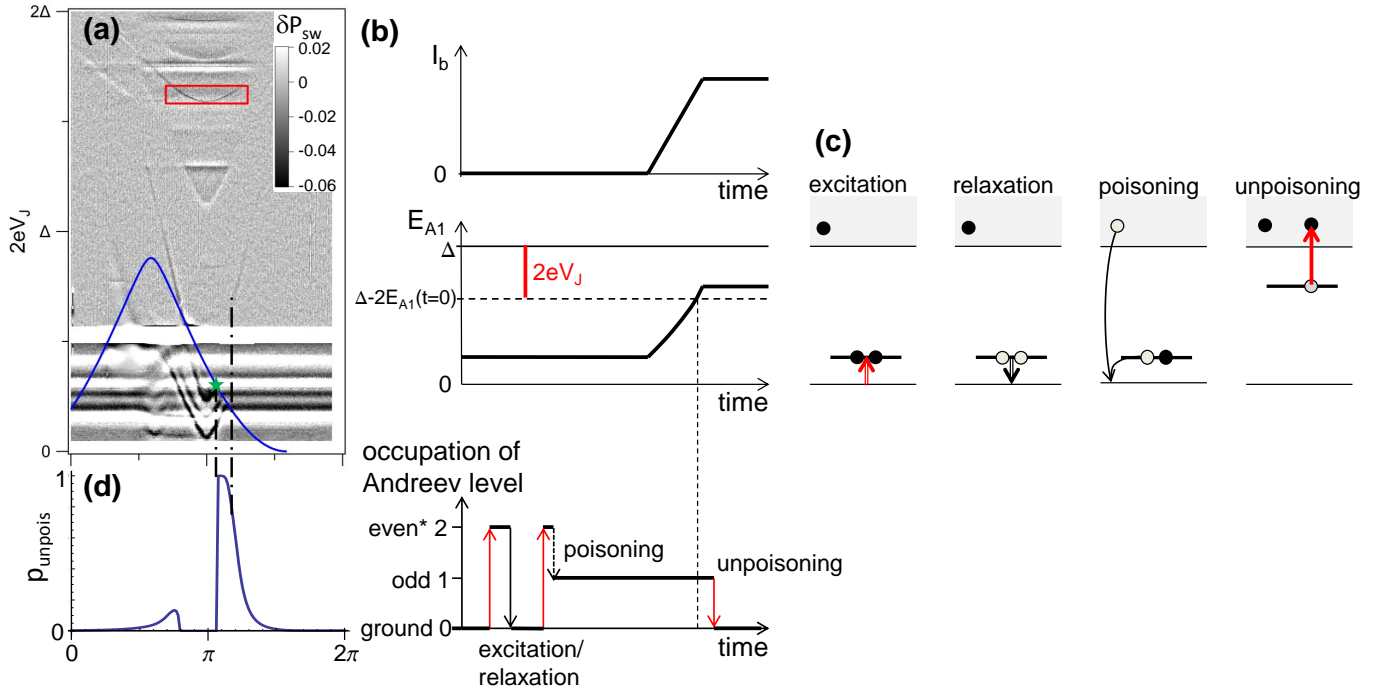
Figure 8: **(a)** Switching spectrum and threshold $2eV_J = \Delta - E_{A1}(\varphi + \gamma_{\mathrm{sw}})$ (blue line) for the excitation of a quasiparticle from the Andreev level to the continuum during the measurement pulse (red box indicates region zoomed in Fig. 9). The green star signals the position where the Andreev transition line $2eV_J = 2E_{A1}$ suddenly disappears. **(b)** Sketch of the evolution of the system when biased resonantly with the Andreev transition, at a position just next to the green star, above the blue line ($2eV_J = 2E_{A1}\,(1.1\pi)$). Top: bias current of the SQUID, just before and at the beginning of a measurement pulse; middle: time evolution of the Andreev energy E_{A1}, which changes because the phase across the contact is $\delta = \varphi + \gamma_{\mathrm{sw}} \simeq \varphi + \arcsin(I_b/I_0)$; bottom: typical evolution of the occupation of the Andreev level. **(c)** Processes at play. Before the measurement pulse, the system cycles between ground and even excited state, through excitation (induced by the excitation at energy $2E_{A1}$) and relaxation processes. At some point, poisoning occurs: the Andreev doublet becomes singly occupied. During the measurement pulse, E_{A1} increases, and when it reaches $\Delta - 2E_{A1}(t=0)$ (vertical dashed line) the energy of the photons from the emitter is sufficient to excite the quasiparticle from the Andreev level to the continuum, and the Andreev system can return to its ground state (unpoisoning). **(d)** Numerical evaluation of p_{unpois}, the unpoisoning probability during measurement.
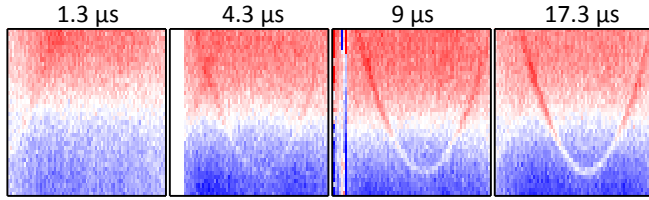

Figure 9: Spectroscopy Andreev transition of the second channel ($2eV_J = 2E_{A2}$) near $\varphi = \pi$, with increasing delay Δt between prepulse and measurement pulse (1.3 to 17.3 μs). In each sub-spectrum, the x-axis spans the interval $0.7\pi < \varphi < 1.3\pi$, the y-axis $1.58\Delta < 2eV_J < 1.66\Delta$ (red box in Fig. 8(a)).

[1] B.D. Josephson, *Possible new effects in superconductive tunnelling*, Phys. Lett. **1**, 251 (1962).

[2] C.W.J. Beenakker, *Universal limit of critical-current fluctuations in mesoscopic Josephson junctions*, Phys. Rev. Lett. **67**, 3836 (1991).

[3] Philip F. Bagwell, *Suppression of the Josephson current through a narrow, mesoscopic, semiconductor channel by a single impurity*, Phys. Rev. B **46**, 12573 (1992).

[4] L. Bretheau, Ç. Ö. Girit, H. Pothier, D. Esteve and C. Urbina, *Exciting Andreev pairs ina superconducting atomic contact*, Nature **499**, 312 (2013).

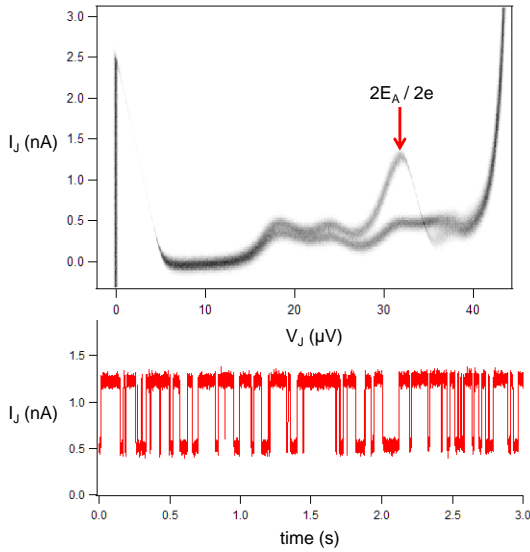[5] L. Bretheau, PhD thesis (2012), *Localized excitations*

Figure 10: Top: Multiple traces of the current-voltage characteristic of the emitter junction coupled to an atomic contact with a channel with transmission 0.97, at $\varphi \sim \pi$, showing bistability. Bottom: time dependence of the current I_J through the emitter biased at $V_J = 2E_A/2e$ (red arrow in top panel). The current is high when the system cycles between ground and even excited state, and low in an odd state.

in superconducting point contacts: probing the Andreev doublet. Available on-line at http://pastel.archivesouvertes.fr/pastel-00862029.

[6] F. S. Bergeret, P. Virtanen, T. T. Heikkilä, and J. C. Cuevas, *Theory of Microwave-Assisted Supercurrent in Quantum Point Contacts,* Phys. Rev. Lett. **105**, 117001 (2010).

[7] F. S. Bergeret, P. Virtanen, A. Ozaeta, T. T. Heikkilä, and J. C. Cuevas, *Supercurrent and Andreev bound state dynamics in superconducting quantum point contacts under microwave irradiation,* Phys. Rev. B **84**, 054504 (2011).

[8] F. Kos, S. E. Nigg, and L. I. Glazman, *Frequency-dependent admittance of a short superconducting weak link,* Phys. Rev. B **87**, 174521 (2013).

[9] Michel H. Devoret, Daniel Esteve, John M. Martinis, Andrew Cleland, and John Clarke, *Resonant activation of a Brownian particle out of a potential well: Microwave-enhanced escape from the zero-voltage state of a Josephson junction,* Phys. Rev. B **36**, 58 (1987).

[10] M. Fuechsle, J. Bentner, D. A. Ryndyk, M. Reinwald, W. Wegscheider, and C. Strunk, *Effect of Microwaves on the Current-Phase Relation of Superconductor–Normal-Metal–Superconductor Josephson Junctions,* Phys. Rev. Lett. **102**, 127001 (2009).

[11] J. J. A. Baselmans, A. F. Morpurgo, B. J. van Wees, and T. M. Klapwijk, *Reversing the direction of the supercur-*

[12] B. Dassonneville, M. Ferrier, S. Guï¿œron, and H. Bouchiat, *Dissipation and Supercurrent Fluctuations in a Diffusive Normal-Metal–Superconductor Ring,* Phys. Rev. Lett. **110**, 217001 (2013).

[13] Such junctions, with have a large number of Andreev levels, are described quasi-classically in terms of a continuum of sub-gap states and a continuous occupation function.

[14] M. Zgirski, L. Bretheau, Q. Le Masne, H. Pothier, D. Esteve, and C. Urbina, *Evidence for Long-Lived Quasiparticles Trapped in Superconducting Point Contacts,* Phys. Rev. Lett. **106**, 257003 (2011).

[15] J. M. van Ruitenbeek, A. Alvarez, I. Piï¿œeeyro, C. Grahmann, P. Joyez, M. H. Devoret, D. Esteve, and C. Urbina, *Adjustable nanofabricated atomic size contacts*, Rev. Sci. Instrum. **67**, 108 (1996).

[16] M.L. Della Rocca, M. Chauvin, B. Huard, H. Pothier, D. Esteve, and C. Urbina, *Measurement of the Current-Phase Relation of Superconducting Atomic Contacts*, Phys. Rev. Lett. **99**, 127005 (2007).

[17] D. Vion, A. Aassime, A. Cottet, P. Joyez, H. Pothier, C. Urbina, D. Esteve, and M.H. Devoret, *Manipulating the Quantum State of an Electrical Circuit*, Science **296**, 886 (2002).

[18] See section VI.Supplemental Material.

[19] Measurements on another contact showed that this structure shifted to lower voltages when longer measurement pulses were applied. This is compatible with the current dependence of the plasma frequency $\nu_p \propto (1 - I_b/I_0)^{1/4}$, since switching occurs at smaller values of I_b when longer pulses are used.

[20] Moreover, when $0.55\pi < \varphi < 1.15\pi$, $2E_{A1}(\varphi + \gamma)$ crosses the plasma energy $h\nu_p(I_{sw})$ during the rise-time of the pulse. Since the excited Andreev state and the plasma mode are strongly coupled [4], and since the lifetime of the plasma mode is in the ns range, this crossing causes relaxation to the ground state.

[21] D.G. Olivares, A. Levy Yeyati, L. Bretheau, ï¿œœe. ï¿œœe. Girit, H. Pothier, and C. Urbina, *Dynamics of quasiparticle trapping in Andreev levels*, arXiv:1309.7283 (2013).

[22] Transitions in the opposite direction are not represented because their rates are much smaller [14, 21].

[23] Although numerical evaluations of the rate for this unpoisoning process using Ref. [8] are an order of magnitude too small to validate this hypothesis.

[24] J-D. Pillet, C. H. L. Quay, P. Morfin, C. Bena, A. Levy Yeyati and P. Joyez, *Andreev bound states in supercurrent-carrying carbon nanotubes revealed*, Nature Phys. **6**, 965 (2010).

[25] N. M. Chtchelkatchev and Yu.V. Nazarov, *Andreev Quantum Dots for Spin Manipulation*, Phys. Rev. Lett. **90**, 226806 (2003).

[26] C. Padurariu and Yu. V. Nazarov, *Spin blockade qubit in a superconducting junction*, EPL **100**, 57006 (2012).